Synthesis of Single-Wall Carbon Nanotubes by Excimer Laser Ablation

P. M. Bota[a], D. Dorobantu[a], I. Boerasu[a], D. Bojin[a], M. Enachescu[b]

[a]Center for Surface Science and Nanotechnology – University Politehnica of Bucharest, 313 Splaiul Independentei, Bucharest, Romania, e-mail: marius.enachescu@upb.ro
[b]Academy of Romanian Scientists, 125, Calea Victoriei, sector 1, RO – 010071, Bucharest, Romania

We report the KrF excimer laser ablation of carbonaceous targets in an innovative laser ablation chamber. The targets have been prepared using a new approach, without pressing or hot pressing of the composition. The Co/Ni doped target has yielded single-wall carbon nanotubes with a narrow diameter distribution. High-resolution transmission electron microscopy has been used along with the confocal Raman microscopy to characterize the products obtained. Thermogravimetric analysis confirms the presence of multiple carbonaceous species with different oxidation temperatures.

Keywords: single-wall carbon nanotubes, laser ablation, transmission electron microscopy, Raman spectroscopy.

УДК 544.1:54.057:54.058

INTRODUCTION

Carbon nanotubes and in particular single-wall carbon nanotubes (SWCNTs) have been the subject of intensive research since their discovery in the early 1990s [1, 2]. The techniques used for the SWCNTs synthesis include arc-discharge [1, 2], chemical vapor deposition (CVD) [3] and laser vaporization [4]. Pulsed Laser Vaporization (PLV) is considered to yield SWCNTs of high quality and high purity. The optimization of PLV technique for the SWCNTs synthesis has been studied in terms of the laser wavelength, ablation temperature, the working gas or the ablated target composition [4–6].

The influence of the wavelength on the graphite laser ablation has been studied via measuring the distribution of carbon clusters in the ablation plume by Gaumet *et al.* [7]. A shorter wavelength produces smaller and faster carbon clusters. The yield of ablation has been shown to increase with the decrease of the wavelength but to drop in the UV range [7]. This can be explained by taking into account the photoelectric effect when the photon energy is higher than the graphite work function.

In this work we report a successful preparation of SWCNTs with a narrow diameter distribution using laser ablation with a KrF, 248 nm wavelength, excimer laser. The ablation chamber implemented in our laboratory has a novel design and applies a new target preparation method that does not use pressing or hot pressing of the target.

EXPERIMENTAL

The ablation of the carbonaceous targets has been carried out in a custom-designed laser ablation chamber. Figure 1 presents a schematic design of this chamber. It consists of a 1260 mm long quartz tube, 60 mm in diameter, placed inside an electrical oven. The 675 mm long oven can control the temperature in the 30–1200°C range.

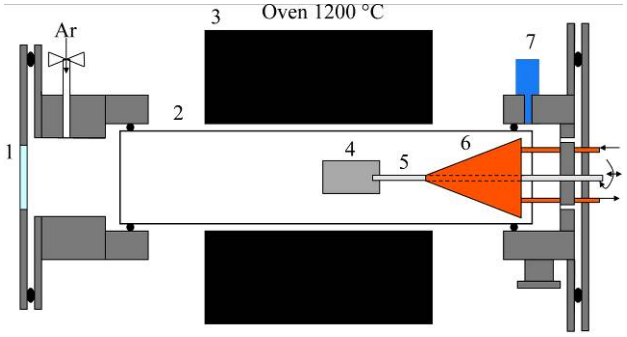

Fig. 1. Chamber schematics: 1 – Quartz laser window; 2 – Quartz tube; 3 – Electrical Oven; 4 – Target; 5 – Graphite transfer rod; 6 – Cold Finger; 7 – Vacuum gauge.

As the growth of the carbon nanotubes is influenced by the oven temperature [8], the quartz tube and the oven have been doubled compared to previous designs [4, 5] to ensure a more uniform temperature inside the ablation reactor.

The laser employed in these experiments has been a KrF excimer laser, working at 248 nm with a pulse length of 25 ns. The laser energy can be varied from 200 mJ to 700 mJ. The pulse frequency can also be varied from 1 to 50 Hz. The laser beam has been focused on a 20 mm^2 spot on the target.

The target, 20 mm in diameter, sits inside the quartz tube, mounted on a graphite rod through which a circular motion is imprinted ensuring a uniform ablation.

The pressure of the ablation carrying gas, Argon 99.96%, can be controlled by a vacuum pump between 10 and 760 Torr. The flow of the ablation carrying gas can also be varied between 0 and 300 L/h. The ablation gas flows from the inlet, just behind the quartz window, downstream to a copper,

water cooled collector. The collector has been elongated to 260 mm to ensure a large surface for the ablation products to condense. Figure 2 shows an image of an elongated cold finger in comparison with a shorter, previously used one. The longer cold finger also induces a smaller temperature gradient over its length.

Fig. 2. Photographs of new and previous designed cold fingers. The length ratio of the new cold finger vs. an older design is over 4.5:1.

The targets utilized were prepared by mixing graphite cement supplied by Metal Forming Lubricants Inc. with Cobalt and Nickel powders. The powders were supplied by Sigma Aldrich, with the particle sizes <1μm for Ni and ~ 2 μm for Co. The compositions investigated were: 98.8 at% C, 0.6 at% Co and 0.6 at% Ni. The cement-catalyst mixture has been introduced in a Teflon mold and heated to 130^{o}C for 4 hours. Then the target was heated to 800^{o}C for 1 hour in an inert atmosphere to ensure the complete removal of any organic compound.

The ablation reactor was heated to 1100^{o}C under the argon pressure and the flow controlled to 500 Torr and 200 L/h. The laser pulse energy was 700 mJ and the frequency 30 Hz.

The ablation products were collected from their deposit onto the water cooled collector and investigated as such by the High-Resolution Transmission Electron Microscopy (HRTEM), confocal Raman microscopy and Thermogravimetric Analysis (TGA).

RESULTS AND DISCUSSIONS

Characterization by Transmission Electron Microscopy

Figure 3 shows typical Transmission Electron Microscopy (TEM) micrographs of the unprocessed products collected after ablation. The raw products were dispersed in ethanol in an ultrasonic bath for 15 minutes. The micrographs were obtained using a JEOL-ARM200F TEM with a 200 kV acceleration voltage. The SWCNTs are found in bundles or individually along with amorphous carbon and metal catalyst particles. The diameters of individual nanotubes have been estimated to be between 0.91 nm and 1.46 nm. Similar values have been reported by other authors for the SWCNTs obtained by laser ablation of targets with a similar composition [5]. The length of the SWCNTs can be of several μm, with the ends usually buried in the amorphous carbon.

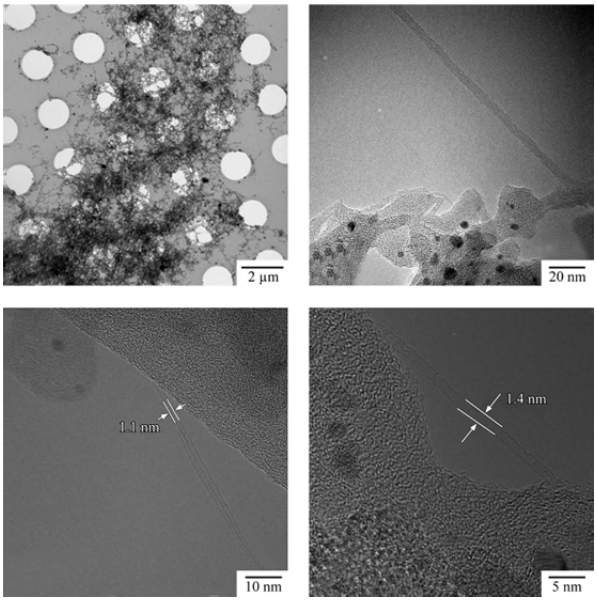

Fig. 3. HRTEM micrographs of ablation products.

The size of the catalyst particles has also been estimated using HRTEM micrographs. The diameters have been found to be between 2 and 15 nm, with a mean diameter of 3 nm. The HRTEM micrographs indicate that the catalyst particles are larger, confirming the sea-urchin-type structure of shorter SWCNTs [8].

CHARACTERIZATION BY CONFOCAL RAMAN MICROSCOPY

The products obtained have also been characterized by the confocal Raman microscopy with a Horiba Labram 800, using 532 nm and 633 nm excitation wavelengths. The spectra of the ablation products were recorded and compared to those of commercial SWCNTs from Sigma Aldrich. Three bands are present in the spectra: the first, in the 100 cm^{-1} to 300 cm^{-1} range, is called the Radial Breathing Mode (RBM), the second band, centered around 1340 cm^{-1}, is called the D band and the third, in the 1500 cm^{-1} to 1650 cm^{-1} region, is called the G band.

Figure 4 presents the spectra obtained in the 100 cm^{-1} to 300 cm^{-1} range at both wavelengths for the products synthesized and for commercial SWCNTs from Sigma Aldrich. The RBM is characteristic for vibrations in the radial direction; this frequency is strongly dependent on the diameter of the nanotubes [9]. The equation that describes the proportionality of the ω_{RBM} to the inverse of the diameter is:

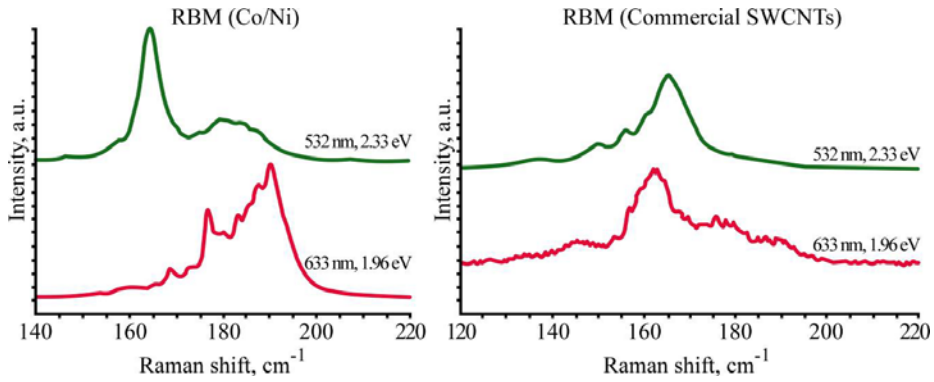

Fig. 4. Raman spectra in RBM region for ablation products and commercial SWCNTs with a 532 nm and 633 nm excitation wavelength.

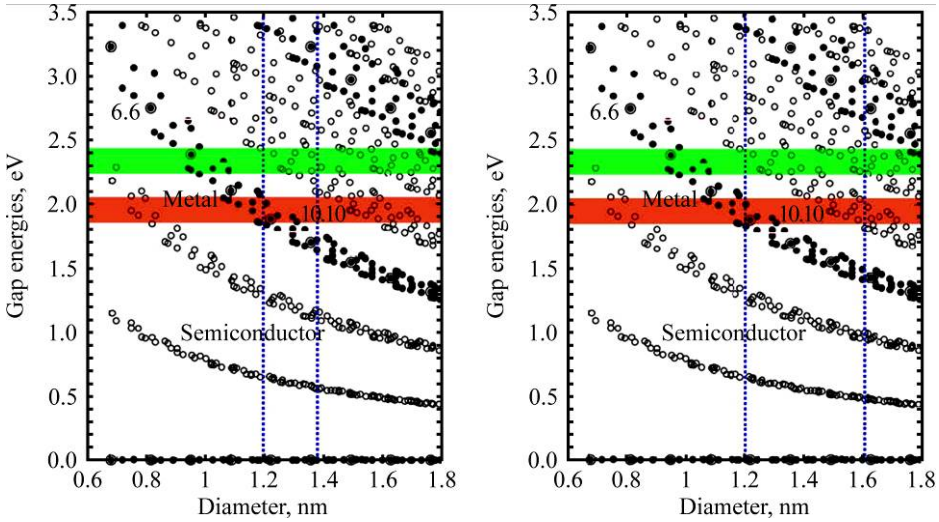

Fig. 5. Kataura plot with hollow circles indicating semiconductor nanotubes and black dots indication metallic nanotubes. The horizontal light grey and dark grey rectangles indicate the regions centered at 1.96 eV and 2.33 eV. The vertical dotted lines are the diameter distribution (estimated from RBM frequencies) limits for our ablation products on the left and commercial SWCNTs on the right.

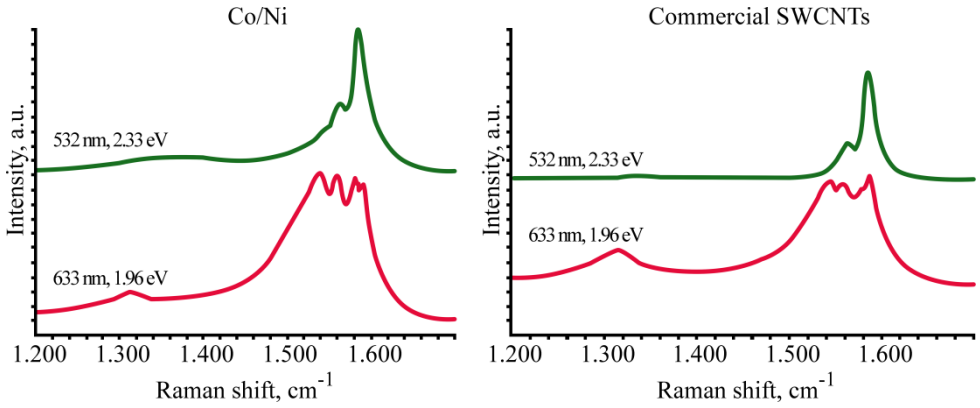

Fig. 6. High frequency region of Raman spectra for our ablation products on the left and commercial SWCNTs on the right.

$$\omega_{RBM} = \frac{c_1}{d} + c_2$$

where ω_{RBM} is the frequency in the Raman spectrum, d is the diameter of the nanotube and c_1 and c_2 are constants with the values: c_1 = 215 cm^{-1} and c_2 = 18 cm^{-1} [9].

Rao *et al*. have shown that the Raman spectrum at a given wavelength is strongly influenced by the resonance Raman effect [10]. The features present are enhanced if the energy of the excitation photons is close to the energy of an electronic transition in the nanotube. Kataura and colleagues have calculated and plotted the dependency of transition energies as a function of the diameter [11]. Using their plot, the metallic or semiconductor character of the nanotubes that show the resonance Raman effect for the specific wavelength can be easily identified.

Figure 5 depicts the so-called Kataura plot, with vertical dotted lines indicating the limits of the diameter distribution, as estimated with the above

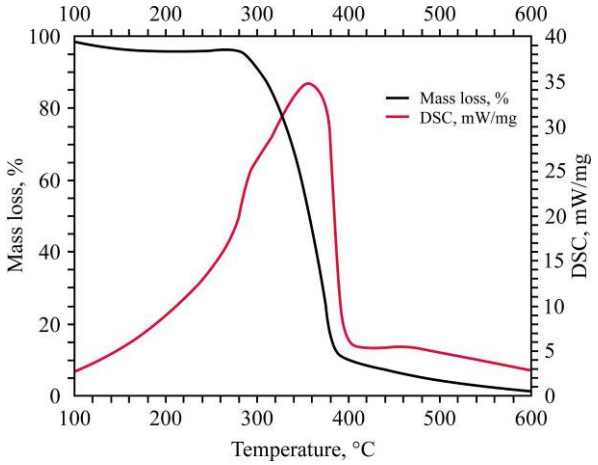

Fig. 7. TGA and DSC curves for ablation products from the Co/Ni doped target.

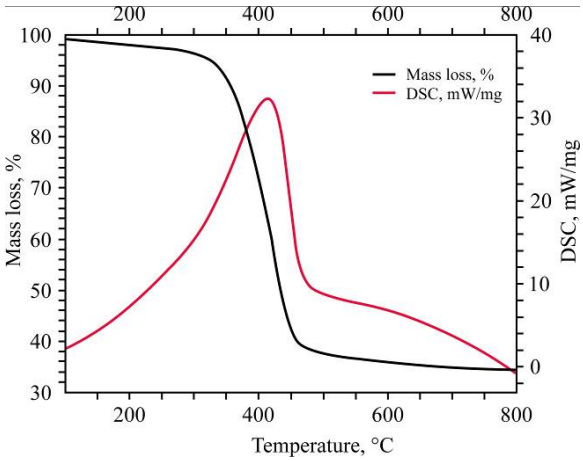

Fig. 8. TGA and DSC curves for commercial SWCNTs.

equation, of the SWCNTs synthesized and the distribution of the commercial SWCNTs. The red and green horizontal rectangles indicate the regions centered at 1.96 eV and 2.33 eV, respectively. The graph clearly shows that for the ablation products, using the 633 nm wavelength, only metallic nanotubes will show the resonance Raman effect. The commercial SWCNTs that show the resonance Raman effect for this wavelength are both metallic and semiconducting. For the 532 nm wavelength however, both samples contain only nanotubes with semiconductor character that show the resonance Raman effect.

The regions in the Raman spectra between 1300 cm^{-1} and 1700 cm^{-1} show the presence of the D and G bands. The D band is characteristic for scattering on sp^3 hybridized carbon atoms. The Raman signal in the D band is given by both amorphous carbon in the sample and defects in the nanotubes. The G band is specific for scattering on sp^2 carbon atoms [9]. The Raman spectra in this region are presented in Fig. 6.

As is clear from this Figure, in the 532 nm spectra of both our Co/Ni ablation products and commercial SWCNTs the G band is split into a G^- band and G^+ band. The G^- band is centered at 1562 cm^{-1} and the G^+ band is centered at 1585 cm^{-1}. The G^- band is characteristic for vibrations in the circumferential direction and G^+ is characteristic for vibrations along the nanotube axis. The ratio of the intensities of these two bands is a good indication of the character of the SWCNTs from the sample [12].

The spectra in Fig. 6 clearly demonstrate a high ratio of intensities $I_{G}+/I_{G}-$ for the spectra taken with the 532 nm excitation wavelength for both the ablation products of the Co/Ni doped target and the commercial SWCNTs.

The Raman spectrum of the ablation products, taken with the 633 nm excitation wavelength, shows the G^- band centered at 1536 cm^{-1} and the G^+ band at 1581 cm^{-1}. The Raman spectrum of the commercial SWCNTs shows the G^- band centered at 1545 cm^{-1} and the G^+ band at 1586 cm^{-1}. The increase in the G^-/G^+ intensity ratio is a result of the resonance Raman effect in metallic nanotubes. This is in good agreement with the information obtained from the so-called Kataura plot.

A comparison of the Raman spectra between the SWCNTs synthesized in our laboratory and the commercial SWCNTs shows that the obtained products have a smaller diameter distribution than the commercial nanotubes. This is evident from the spectra in the RBM region. As the Raman frequency of the G band is less influenced by the diameter of the SWCNTs we can see the similarity of the spectra in the 1300–1700 cm^{-1} region. This similarity of the G bands from the spectra indicates that the ratio of metallic to semiconductor nanotubes is comparable in the two samples.

THERMOGRAVIMETRIC ANALYSIS

The TGA and DSC curves in Figs. 7 and 8 have been obtained by heating the sample at 5°C/min in air. The weight loss and heat released indicates that multiple carbon species are present in both our ablation products and the commercial SWCNTs. Most of the oxidation of the sample takes place between 297°C and 400°C for the ablation products and between 350°C and 450°C for the commercial SWCNTs. The oxidation temperature of SWCNTs has been shown to be strongly influenced by the presence of amorphous carbon [13]. Further purification by oxidation of the products will be carried out in order to obtain SWCNTs with high purity.

CONCLUSIONS

Single-wall carbon nanotubes have been obtained by laser ablation of Co/Ni doped targets using our new chamber design and a KrF excimer laser. The SWCNTs obtained via the new chamber design have a narrower diameter distribution than the commercial ones, between 1.2 nm and 1.4 nm.

The target preparation method that excludes the need of pressing or hot pressing has been proven to be suitable for obtaining laser ablation targets.

The composition of the ablation products has been investigated by HRTEM, confocal Raman microscopy and TGA. The SWCNTs obtained by laser ablation are embedded along metal catalyst nanoparticles in amorphous carbon. The method is suitable for obtaining both metallic and semi-conducting SWCNTs, as indicated by the resonance Raman spectroscopy.

ACKNOWLEDGMENTS

This work was supported by the Ministry of Education, Research, Youth and Sport of Romania, by the European Union through the European Regional Development Fund, and by the Romanian National Authority for Scientific Research, under project POSCCE-O 2.1.2-2009-2/12689/717. This paper was supported by the "Doctoral Scholarships investing in research development innovation for the future (DOCINVEST)" POSDRU\107\1.5\S\76813.

Authors express their gratitude to Dr. Eng. Ovidiu Oprea from University POLITEHNICA of Bucharest for the TGA measurements.

REFERENCES

1. Iijima S. Helical Microtubes of Graphitic Carbon. *Nature.* 1991**, 354**, 56–58.
2. Bethune D.S., Kiang C.H., deVries M.S., Gorman G., Savoy R., Vasquez J. and Beyers R. Cobalt-catalysed Growth of Carbon Nanotubes with Single-atomic-layer Walls. *Nature.* 1993, **363**, 605–607.
3. Endo M., Takeuchi K., Kobori K., Takahashi K., Kroto H.W. and Sarkar A. Pyrolitic Carbon Nanotubes from Vapour-grown Carbon Fibers. *Carbon.* 1995, **33**, 873–881.
4. Guo T., Nikolaev P., Thess A., Colbert D.T. and Smalley R.E. Catalytic Growth of Single-walled Nanotubes by Laser Vaporization. *Chem Phys Lett.* 1995, **243**, 49–54.
5. Braidy N., El Khakani M.A. and Botton G.A. Single-wall Carbon Nanotubes Synthesis by Means of UV Laser Vaporization. *Chem Phys Lett.* 2002, **354**, 88–92.
6. Le Borgne V., Aissa B., Mahomedi M., Kim Y.A., Endo M. and El Khakani M.A. Pulsed KrF-laser Synthesis of Single-wall-carbon-nanotubes: Effects of Catalyst Content and Furnace Temperature on their Nanostructure and Photoluminescence Properties. *J Nanopart Res*. 2011, **13**, 5759–5767.
7. Gaumet J.J., Wakisaka A., Shimizu Y. and Tamori Y. Energetics of Carbon Clusters Produced Directly by Laser Vaporization of Graphite: Dependence on Laser Power and Wavelength. *J Chem Soc Faraday Trans*. 1993, **89**, 1667–1670.
8. Kataura H., Kumazawa Y., Maniwa Y., Ohtsuka Y., Sen R., Suzuki S. and Achiba Y. Diameter Control of Single-walled Carbon Nanotubes. *Carbon.* 2000, **38**, 1691–1697.
9. Maultzch J., Teig H., Reich S. and Thomsen C. Radial Breathing Mode of Single-walled Carbon Nanotubes: Optical Transition Energies and Chiral-index Assignment. *Phys Rev Lett*. B. 2005, **72**, 205438–205454.
10. Rao M., Richter E., Bandow S., Chase B., Eklund P.C., Williams K.A., Fang S., Subbaswamy K.R., Menon M., Thess A., Smalley R.E., Dresselhaus G., and Dresselhaus M.S. Diameter-Selective Raman Scattering from Vibrational Modes in Carbon Nanotubes. *Science.* 1997, **275**, 187–191.
11. Kataura H., Kumazawa Y., Maniwa Y., Umezu I., Suzuki S., Ohtsuka Y., Achiba Y. Optical Properties of Single-Wall Carbon Nanotubes. *Synth Met*. 1999, **103**, 2555–2558.
12. Jorio A., Dresselhaus G., Dresselhaus M.S., Souza M., Dantes M.S.S., Pimenta M.A., Rao A.M., Saito R., Liu C. and Cheng H.M. Polarized Raman Study of Single-Wall Semiconducting Carbon Nanotubes. *Phys Rev Lett*. 2000, **85**, 2617–2620.
13. Rinzler A.G., Liu J., Dai H., Nikolaev P., Huffman C.B., Rodrıguez-Macıas F.J., Boul P.J., Lu A.H., Heymann D., Colbert D.T., Lee R.S., Fischer J.E., Rao A.M., Eklund P.C. and Smalley R.E. Large-scale Purification of Single-wall Carbon Nanotubes: Process, Product, and Characterization. *Appl Phys A.* 1998, **67**, 29–37.

Received 15.04.13
Accepted 03.05.13

Реферат

Сообщается об абляции углеродистой мишени с помощью эксимерного KrF лазера в инновационной абляционной камере. Мишень подготовлена с использованием нового подхода без применения прессования или горячего прессования композиции. Co/Ni-легированная мишень привела к получению одностенных углеродных нанотрубок с малым разбросом диаметров. Электронная трансмиссионная микроскопия высокого разрешения наряду с конфокальной Рамановской микроскопией использованы для характеризации полученных продуктов. Термогравиметрический анализ подтверждает присутствие множества углеродистых образцов с различными температурами окисления.

Ключевые слова: одностенные углеродные нанотрубки, лазерная абляция, электронная трансмиссионная микроскопия, Рамановская спектроскопия.